International Journal of Control, Automation and Systems 15(6) (2017) 2871-2882
http://dx.doi.org/10.1007/s12555-016-0492-x
ISSN:1598-6446 eISSN:2005-4092
http://www.springer.com/12555

Stable Assist-as-needed Controller Design for a Planar Cable-driven Robotic System

Hamed Jabbari Asl and Jungwon Yoon*

Abstract: Robot-assisted rehabilitation systems have shown promising advantages over traditional therapist-based methods. The type of the controller has an important role in the efficiency of such systems. In this regard, this paper presents a new assist-as-needed (AAN) controller for 4-cable planar robots. The main purpose is to design a bounded-input AAN controller with an adjustable assistance level and a guaranteed closed-loop stability. The proposed controller involves the advantages of both the model-based and non-model-based AAN controllers, and in this way can increase the efficiency of rehabilitation. The controller aims to follow a desired trajectory by allowing an adjustable tracking error, which enables the human subject to freely move the target limb inside this error area. This feature of the controller gives an important advantage over the existing model-based controllers. The controller also compensates for the dynamic modeling uncertainties of the system through an adaptive neural network. The adaptive term includes a forgetting factor to adjust the assistance level of neural network term. The stability of the closed-loop system is analysed, and the uniformly ultimately bounded stability is proven. The effectiveness of the proposed control scheme is validated through simulations conducted for gait rehabilitation.

Keywords: Adaptive control, assist-as-needed control, neural network, parallel robot, rehabilitation.

1. INTRODUCTION

Patients with neurological injuries, which are primarily caused by stroke, suffer from serious muscle weakness. Limitation in movement of the both upper and lower limbs is a prevalent problem in such patients. Physical therapy, including rehabilitation, has been proven to have significant impact on the recovery of these patients. In this regard, intensive training is noted to be a crucial factor to achieve an effective rehabilitation [1]. Such training usually includes the repetition of a movement which involves the muscles affected by the neurological injury. Robotic training systems have shown great advantages over the traditional methods, which are performed manually by physiotherapists [2]. These systems can facilitate repetitive training for longer duration, and provide useful information for post-processing and analysis from the attached onboard sensors. The robotic systems can be applied in assistive, challenge-based, simulation, and coaching strategies [3].

One classification for training robots is done based on the structure of the robot. In this view, the robots are classified as either exoskeleton type or end-effector type [4]. In the first type, the robot covers the target limb and applies a force to several segments of it, while in the end-effector type, there is only a single interface between the robot and the subject. In another classification, they are considered as either active, where the robot's active actuators apply a force to move the limb, or passive, where a human subject moves the limb with passive support of the robot [5]. Most recent assistive robotic systems are equipped with actuators, since they are easily programmable and give versatile functionality to adapt for different human subjects with various levels of injury. For example, in [6] a treadmill-based robotic training system is developed for gait rehabilitation. A similar commercialized system is Lokomat [7]. A cable-driven arm exoskeleton is introduced in [4]. Pneu-WREX is another robotic orthosis for re-training arm movement [8].

Controller design is one of the main challenges of developing assistive robots. The type of controller plays an important role in the efficiency of the system in increasing the patient recovery. One approach to deal with this issue is to design a stiff controller for the robot to follow a predetermined movement pattern, such that the patient is not allowed to have active participation to achieve an appropriate pattern. Although this method is effective in the early stages of treatment for the patients with high level of

Manuscript received August 4, 2016; revised November 26, 2016 and February 8, 2017; accepted February 17, 2017. Recommended by Associate Editor Changchun Hua under the direction of Editor Fuchun Sun. This work was supported by the National Research Foundation Korea (NRF) (2014R1A2A1A11053989 & 2017R1A2B4011704) and Dual Use Technology Program of Civil and Military.

Hamed Jabbari Asl is with Control System Laboratory, Toyota Technological Institute, Nagoya, Japan (e-mail: hjabbari@gnu.ac.kr). Jungwon Yoon is with School of Integrated Technology, Gwangju Institute of Science and Technology, Gwangju, Korea (e-mail: jyoon@gist.ac.kr).
* Corresponding author.

injury, the outcomes of the research in [9] reveal that this approach, however, is less effective in the next stages comparing to the traditional treatments by physiotherapists.

One approach to solve the aforementioned problem is to allow the patient to attempt for the movement beside the assistance of the robot. In the literature, this method is called “assist-as-needed" (AAN), and refers to the control strategies in which the output of the controller becomes smaller when the human subject can follow the desired movement pattern [5, 7, 10–13]. First effort in applying such algorithm was the use of impedance controller [7]. An AAN controller is also reported in [5] for gait rehabilitation. In this research, a virtual wall is defined around the desired gait pattern and the robot tries to keep the patient’s foot inside a tunnel defined by the wall. The controller includes a gravity compensation term, and some intuitive terms to generate an adjustable virtual wall, where the wide of the tunnel defines the level of freedom of the patient in generating the movement. A similar approach is tested and validated on mice [12], and followed in [14] with considering a path control problem.

In order to guarantee the stability of the AAN systems in the presence of dynamic modeling uncertainties, [15] has proposed a model-based adaptive AAN controller. This controller includes a proportional-derivative (PD) impedance controller with an adaptive term to compensate for the unknown parametric uncertainties of the system, which mainly include the gravity information. The adaptation law involves a forgetting factor, which decreases the imposed assistance by the adaptive term when the tracking error of the desired gait pattern is small, leading to an AAN performance. Another adaptive model-based controller is proposed in [16] for arm rehabilitation. To achieve an AAN property, the controller is designed such that the closed-loop system is uniformly ultimately bounded; i.e., the tracking error converges to a close neighborhood of the origin.

In the above-mentioned model-based controllers, the PD term usually produces the main output of the controller. This term is zero only when the tracking error is zero, which generally does not happen in practice, and linearly increases, with a slope defined by the control gains, as the error increases . Consequently, the concept of “freedom tunnel", existing in non-model-based approaches, is not fully satisfied in these model-based controllers. Also, in these controllers, the regressor matrix is required to derive an adaptive law for parameter estimation. This matrix is usually difficult to determine in practice, and hence, Gaussian radial basis functions are utilized to estimate it; however, the estimation error is not taken into account in the stability analysis. Moreover, the structure of the controllers are not *a priori* bounded, which means that the saturation level of the actuators are not considered is the stability analysis.

Cable-driven parallel robots (CDPRs) are a class of parallel robotic manipulators, in which the end-effector is moved by means of cables. In such systems, the cables are attached to fixed actuators in one end and to the end-effector in the other end, which can change the length of the cables and pose of the end-effector accordingly [17, 18]. These robots introduce many advantages over exoskeleton robots for rehabilitation [19]. For example, they are too much lighter and have low movement inertia comparing to the exoskeleton robotic systems. In addition, similar to end-effector-based structures, these robots move the target limb by directly exerting force to the limb, instead of actuating the joints [4]. Motivated by these advantages, many researches have been devoted to the use of CDPRs for rehabilitation; e.g., [20–23].

In this paper, the problem of AAN controller design for planar CDPRs is addressed. The main objective is to develop a theoretical framework for stable bounded-input AAN controller design to follow a predetermined motion trajectory in the presence of uncertainties in the dynamic model of the system. The proposed approach can synthesize the advantages of the model-based and non-model-based AAN controllers in order to achieve a more efficient and robust rehabilitation system. The controller includes a bounded PD-like term with dead-zone area, which, analogous to non-model-based methods, produces a tunnel of freedom for the motion of the target limb inside the dead-zone area. The controller also involves an adaptive neural network (NN) term to compensate for the unknown dynamics of the system. Similar to the existing adaptive model-based AAN controllers, the NN term has a forgetting factor to decrease its output level for small values of tracking error. The stability of the closed-loop system is well studied and the uniformly ultimately bounded stability is guaranteed. Simulation results are presented to show the effectiveness of the controller.

The rest of the paper is organized as follows: Section 2 presents the kinematic and dynamic models of the 4-cable planar robots. The proposed AAN controller is given in Section 3, where also the stability of the system is studied. Section 4 presents simulation results, and finally conclusions are given in Section 5.

2. THE ROBOT AND ITS EQUATIONS OF MOTION

CDPRs have shown interesting advantages over the conventional rigid-link robotic systems for rehabilitation applications. Low mass and inertia are the main motivations to use them as assitive robots. Therefore, in this paper, AAN controller design is studied for a 4-cable planar robot, which can be applied for gait rehabilitation [19].

A schematic diagram illustrating the basic concept of the use of a 4-cable planar parallel robot in treadmill gait rehabilitation is shown in Fig. 1. In this configuration, the shank is considered as the end-effector, and its movement

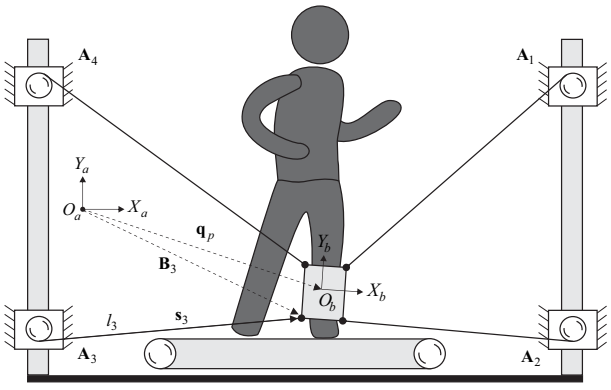

Fig. 1. A configuration of a cable-deriven parallel robot with a treadmill for gait rehabilitation.

on sagittal plane is controlled by four cables. This configuration can generate all possible three degrees of freedom movement in the plane for the end-effector, and the leg accordingly. For the CDPRs, there is a wrench-closure workspace which is defined as a set of feasible poses for the robot, which can be balanced by the tension force of the cables [24]. There is a large literature in extracting the wrench-closure workspace of the CDPRs; see e.g. [25] and the references therein. In this paper, in the study of the controller design for the CDPR, it is assumed that the robot trajectory is inside the wrench-closure workspace.

To describe the equations of motion, as shown in Fig. 1, two coordinate frames are considered, i.e., a base frame $\mathcal{A} \triangleq \{O_a, X_a, Y_a\}$, and a end-effector frame $\mathcal{B} \triangleq \{O_b, X_b, Y_b\}$. The position and orientation of $\mathcal{B}$ with respect to $\mathcal{A}$ are respectively expressed by the vector $\mathbf{q}_p \triangleq [x\ y]^\top$, and the rotation matrix $\mathbf{R} : \mathcal{B} \to \mathcal{A}$ associated to angle ϕ, which is given by

$$\mathbf{R} = \begin{bmatrix} \cos(\phi) & -\sin(\phi) \\ \sin(\phi) & \cos(\phi) \end{bmatrix}.$$

The ith cable is attached to its base at the point $\mathbf{A}_i \triangleq [A_{ix}\ A_{iy}]^\top$, and to the end-effector at the point $\mathbf{B}_i \triangleq [B_{ix}\ B_{iy}]^\top$, both with respect to the $\mathcal{A}$ frame. Based on this notation, the cable length l_i is defined as the distance between $\mathbf{A}_i$ and $\mathbf{B}_i$. By defining ω as the angular velocity, the following relation can be obtained for the time derivatives of the cable lengths [26]:

$$\dot{\ell} = \mathbf{J}[\dot{\mathbf{q}}_p^\top\ \omega]^\top,$$

where $\dot{\ell} \triangleq [\dot{l}_1 \cdots \dot{l}_4]^\top$, and the Jacobian matrix $\mathbf{J} \in \Re^{4\times 3}$ is given by

$$\mathbf{J} \triangleq [\mathcal{L}_1/l_1\ \cdots\ \mathcal{L}_4/l_4]^\top,$$

where $\mathcal{L}_i \triangleq [\mathbf{s}_i^\top\ c_3]^\top \in \Re^{3\times 1}$ for $i = 1, \cdots, 4$, with $\mathbf{s}_i \triangleq \mathbf{B}_i - \mathbf{A}_i \in \Re^2$, and $c_3 \in \Re$ denoting the third element of $\mathbf{c} \triangleq [\mathbf{b}_i^\top\ 0]^\top \times [\mathbf{s}_i^\top\ 0]^\top \in \Re^3$, in which $\mathbf{b}_i \triangleq \mathbf{B}_i - \mathbf{q}_p \in \Re^2$.

Considering $\mathbf{q} \triangleq [x\ y\ \phi]^\top \in \Re^3$ as the generalized coordinates vector for the pose of the end-effector, the dynamic model of the cable-driven robot can be written as [27]

$$\mathbf{M}\ddot{\mathbf{q}} + \mathbf{G} + \mathbf{F}_d\dot{\mathbf{q}} + \mathbf{F}_s(\dot{\mathbf{q}}) + \mathbf{T}_d = \boldsymbol{\tau}_s - \mathbf{J}^\top\boldsymbol{\tau}, \tag{1}$$

where $\boldsymbol{\tau} = [\tau_1 \cdots \tau_4]^\top \in \Re^4$ denotes the vector of tension force, $\boldsymbol{\tau}_s \in \Re^3$ is the applied wrench by the subject, $\mathbf{F}_d \in \Re^{3\times 3}$ is the constant viscous friction coefficient matrix, $\mathbf{F}_s(\dot{\mathbf{q}}) \in \Re^3$ is the Coulomb friction, $\mathbf{T}_d \in \Re^3$ is a time-varying disturbance term, and $\mathbf{M} \in \Re^{3\times 3}$ and $\mathbf{G} \in \Re^3$ are respectively the inertia matrix and gravity vector, which are given by

$$\mathbf{M} \triangleq \begin{bmatrix} m & 0 & 0 \\ 0 & m & 0 \\ 0 & 0 & I \end{bmatrix}, \quad \mathbf{G} \triangleq \begin{bmatrix} 0 \\ mg \\ 0 \end{bmatrix},$$

where m and I are respectively the mass and inertia of the end-effector, and g is the gravity acceleration [28]. The dynamics (1) have the following property.

Property 1: The friction terms can be bounded as

$$\|\mathbf{F}_d\dot{\mathbf{q}} + \mathbf{F}_s(\dot{\mathbf{q}})\| \le \zeta_{f_d}\|\dot{\mathbf{q}}\| + \zeta_{f_s}$$

where $\zeta_{f_d}, \zeta_{f_s} \in \Re$ are positive constants, and $\|\cdot\|$ denotes the Euclidean norm.

Also the following assumption is considered for the dynamic equation (1).

Assumption 1: The unmodeled dynamics and applied torque by the human subject are bounded such that [29,30]

$$\|\mathbf{T}_d(t)\| \le \zeta_d,$$
$$\|\boldsymbol{\tau}_s(t)\| \le \zeta_s,$$

where $\zeta_d, \zeta_s \in \Re^+$ are positive constants.

The cables are driven by rotary motors, whose dynamics are usually compensated through high-gain servo loops to follow the desired torques, having voltage or current as their input.

3. AAN CONTROLLER

In this section, an AAN controller is proposed. First, having a desired motion trajectory, error dynamics are developed, and then an AAN controller is designed to regulate these dynamics. The controller utilizes a smooth saturated function with dead-zone area to generate a "freedom tunnel" around the desired trajectory, and also the controller implements an AAN NN to compensate for unknown dynamics of the system. The stability of the closed-loop system is studied at the end of this section.

3.1. Open-loop dynamics and NN estimation

To design the controller, the error signal $\mathbf{e} = [e_1\ e_2\ e_3]^\top \in \Re^3$ is defined as $\mathbf{e} \triangleq \mathbf{q} - \mathbf{q}_d$, where $\mathbf{q}_d \in \Re^3$ denotes the vector of desired trajectory. The following property is assumed for the desired trajectory.

Assumption 2: The movement pattern of the limb is such that $\mathbf{q}_d(t)$, $\dot{\mathbf{q}}_d(t)$ and $\ddot{\mathbf{q}}_d(t)$ are bounded; i.e., $\mathbf{q}_d(t), \dot{\mathbf{q}}_d(t), \ddot{\mathbf{q}}_d(t) \in \mathcal{L}_\infty$.

By differentiating $\mathbf{e}$ for two times, premultiplying by $\mathbf{M}$, and using (1), the dynamics of the error signal can be written as

$$\mathbf{M}\ddot{\mathbf{e}} = -\mathbf{F}_d\dot{\mathbf{q}} - \mathbf{F}_s(\dot{\mathbf{q}}) - \mathbf{G} - \mathbf{T}_d - \mathbf{M}\ddot{\mathbf{q}}_d + \boldsymbol{\tau}_s - \mathbf{J}^\top\boldsymbol{\tau}. \quad (2)$$

To aid the controller design, the filtered error $\mathbf{r} \in \Re^3$ is defined as follows:

$$\mathbf{r} \triangleq \dot{\mathbf{e}} + \eta\mathbf{e}, \quad (3)$$

where $\eta \in \Re^+$ is a constant adjustable gain. Now, the open-loop tracking error system can be developed by computing the time derivative of (3), and using (2) to obtain the following:

$$\mathbf{M}\dot{\mathbf{r}} = \mathbf{f} - \mathbf{T}_d + \boldsymbol{\tau}_s - \mathbf{J}^\top\boldsymbol{\tau}, \quad (4)$$

where the auxiliary function $\mathbf{f} \in \Re^3$ is defined as

$$\mathbf{f} \triangleq \mathbf{M}(\eta\dot{\mathbf{e}} - \ddot{\mathbf{q}}_d) - \mathbf{F}_d\dot{\mathbf{q}} - \mathbf{F}_s(\dot{\mathbf{q}}) - \mathbf{G}. \quad (5)$$

The expression in (5) can be represented by a single-layer radial basis function NN (RBFNN) over a compact set Ω as [31,32]

$$\mathbf{f}(\mathbf{z}) = \mathbf{W}^\top\boldsymbol{\sigma}(\mathbf{z}) + \varepsilon(\mathbf{z}), \quad (6)$$

where $\mathbf{z}(t) \in \Re^{N_1}$, with $N_1 = 13$, is defined as $\mathbf{z} \triangleq \left[1\ \mathbf{e}^\top\ \dot{\mathbf{e}}^\top\ \dot{\mathbf{q}}_d^\top\ \ddot{\mathbf{q}}_d^\top\right]^\top$, $\mathbf{W} \in \Re^{L\times 3}$ is a bounded constant ideal weight matrix with L denoting the number of neurons, $\varepsilon(\mathbf{z}) \in \Re^3$ is the functional reconstruction error, and $\boldsymbol{\sigma}(\mathbf{z}) \in \Re^L$ is the vector of activation function, which is defined as

$$\boldsymbol{\sigma}(\mathbf{z}) \triangleq [\sigma_1(\mathbf{z})\ \sigma_2(\mathbf{z})\ \cdots\ \sigma_L(\mathbf{z})]^\top$$

with the basis gaussian functions $\sigma_i(\cdot)$ for $i = 1,2,\cdots,L$, given by $\sigma_i(\mathbf{z}) \triangleq \prod_{k=1}^{N_1} e^{-(z_k-\mu_{ik})^2/2p_{ik}}$, where z_k, μ_{ik}, and p_{ik} are, respectively, the k-th components of $\mathbf{z}$, the mean vector $\boldsymbol{\mu}_i \in \Re^{N_1}$, and the corresponding diagonal covariance matrix $\mathbf{P}_i = \text{diag}\{p_{ik}\} \in \Re^{N_1\times N_1}$. The following upper bound can be considered for the weight matrix over the compact set Ω [33,34]

$$\|\mathbf{W}\|_F^2 \triangleq \text{tr}\left(\mathbf{W}^\top\mathbf{W}\right) \le W_B,$$

where $W_B \in \Re^+$ is a positive constant, $\text{tr}(\cdot)$ denotes the trace of a matrix, and $\|\cdot\|_F$ denotes the Frobenius norm of a matrix.

Based on (6), a typical one-layer NN approximation for the function $\mathbf{f}$ is given as [33]:

$$\hat{\mathbf{f}}(\mathbf{z}) \triangleq \hat{\mathbf{W}}^\top\boldsymbol{\sigma}(\mathbf{z}), \quad (7)$$

where $\hat{\mathbf{W}}(t) \in \Re^{L\times 3}$ is the subsequently designed estimate of the ideal weight matrix. Denoting the estimate mismatch for the ideal weight matrix by $\tilde{\mathbf{W}}(t) \in \Re^{L\times 3}$, and defining it as $\tilde{\mathbf{W}} \triangleq \mathbf{W} - \hat{\mathbf{W}}$, one can write the function approximation error as follows:

$$\mathbf{f} - \hat{\mathbf{f}} = \tilde{\mathbf{W}}^\top\boldsymbol{\sigma}(\mathbf{z}) + \varepsilon(\mathbf{z}). \quad (8)$$

Property 2: The following bound can be considered for $\varepsilon(\mathbf{z})$ over the compact set Ω [33,35]:

$$\|\varepsilon(\mathbf{z})\| \le \varepsilon_N,$$

where $\varepsilon_N \in \Re^+$ is a positive constant.

3.2. Controller design

To implement the AAN idea, in this paper the continuous saturated dead-zone function $\tanh(\gamma x^3)$, $\forall x \in \Re$ and $\gamma \in \Re^+$, will be utilized, where the positive constant γ can be used to adjust the dead-zone area. As shown in Fig. 2, when the function is multiplied by a constant positive gain k, the scale of γ/k can be used in the argument of the function to achieve almost the same value as in $\tanh(\gamma x^3)$ in the small neighborhood of the origin, which is denoted in the figure by $\hbar$. In practice, considering the dead-zone of the actuators, this small boundary can be assumed as "zero" output; i.e., when $\tau_i \le \hbar$ ($i = 1\cdots 4$ for the studied robot), the corresponding output force is almost zero. Therefore, the dead-zone area can be defined as $\Omega_D \triangleq \left\{x \middle| \left|\tanh(\gamma x^3)\right| \le \hbar\right\}$. The use of this smooth dead-zone function in the controller will facilitate to add a tunnel of freedom around the desired trajectory, where a subject can arbitrarily move the target limb.

Remark 1: Although the function $\tanh(\gamma x^3)$ is nonlinear, outside the dead-zone area until reaching the saturation level it can be considered as a quasi-linear function. Therefore, in the rehabilitation applications, the feeling of the human subject in interaction with the robot will be more natural in comparision to the use of nonlinear control gains as implemented in [16].

For the case of n-dimensional robot, the function $\text{Tanh}(\gamma\boldsymbol{\varpi}(\cdot))$ will be utilized, where the vector function $\boldsymbol{\varpi}(\cdot)$ is defined as $\boldsymbol{\varpi}(\mathbf{x}) \triangleq \mathbf{x}\odot\mathbf{x}\odot\mathbf{x}$, $\forall\mathbf{x} \in \Re^n$, with $\odot$ denoting the element-wise vector product, and $\text{Tanh}(\mathbf{x})$ is defined as

$$\text{Tanh}(\mathbf{x}) \triangleq [\tanh(x_1)\ \cdots\ \tanh(x_n)]^\top,$$

for all $\mathbf{x} = [x_1\cdots x_n]^\top \in \Re^n$. Inspired from [36], the following properties can be derived for the saturated dead-zone function.

Property 3: $\forall\mathbf{x} \in \Re^n$ and $\gamma \in \Re^+$, $\text{Tanh}(\gamma\boldsymbol{\varpi}(\mathbf{x}))$ has the following properties:

(i) $\|\text{Tanh}(\gamma\boldsymbol{\varpi}(\mathbf{x}))\| \le \sqrt{n}$;
(ii) $\mathbf{x}^\top\text{Tanh}(\gamma\boldsymbol{\varpi}(\mathbf{x})) > 0$, $\forall\mathbf{x} \ne \mathbf{0}$;

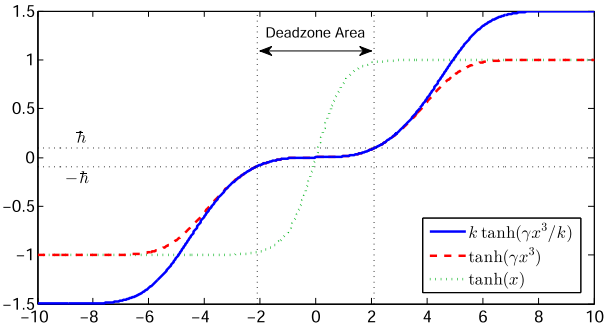

Fig. 2. Deadzone function $k\tanh(\gamma x^3/k)$ (for $\gamma = 0.01$, $k = 1.5$) and its comparison with $\tanh(x)$.

(iii) $\|\mathrm{Tanh}(\gamma\boldsymbol{\varpi}(\mathbf{x}))\| \leq \|\mathbf{x}\|, \forall\gamma < \gamma_M$;
(iv) $\|\mathrm{Tanh}(\gamma\boldsymbol{\varpi}(\mathbf{x}))\|^2 \leq \mathbf{x}^\top \mathrm{Tanh}(\gamma\boldsymbol{\varpi}(\mathbf{x})), \forall\gamma < \gamma_M$;
(v) $\int_{\mathbf{0}}^{\mathbf{x}} \mathrm{Tanh}^\top(\gamma\boldsymbol{\varpi}(\bar{\mathbf{x}}))\mathrm{d}\bar{\mathbf{x}} \to \infty$ as $\|\mathbf{x}\| \to \infty$;
(vi) $\frac{\mathrm{d}}{\mathrm{d}x}\tanh(\gamma x^3) \leq \varepsilon_M < \infty, \forall x \in \Re$;
(vii) $\int_{\mathbf{0}}^{\mathbf{x}} \mathrm{Tanh}^\top(\gamma\boldsymbol{\varpi}(\bar{\mathbf{x}}))\mathrm{d}\bar{\mathbf{x}} \leq \frac{\gamma^{1/3}}{2}\|\mathbf{x}\|^2$;
(viii) $\tanh^2(\frac{\gamma}{n^{3/2}}\|\mathbf{x}\|^3) \leq \|\mathrm{Tanh}(\gamma\boldsymbol{\varpi}(\mathbf{x}))\|^2$;
(ix) $\tanh(\frac{\gamma}{n^{3/2}}\|\mathbf{x}\|^3)\|\mathbf{x}\| \leq \mathrm{Tanh}^\top(\gamma\boldsymbol{\varpi}(\mathbf{x}))\mathbf{x}$,

where $\gamma_M, \varepsilon_M \in \Re^+$ can be obtained, using numerical solutions, as $\gamma_M \simeq 2.01$, and $\varepsilon_M \simeq 1.52\gamma^{1/3}$.

The objective of the controller design is to find the appropriate tension of cables to regulate the dynamics (4) in an AAN way. For these dynamics, it is necessary to have a positive tension in all cables. Therefore, to find the tension vector of the cables, the following general solution is applied, which follows the internal forces concept [18]:

$$\boldsymbol{\tau} = (\hat{\mathbf{J}}^\top)^\dagger \boldsymbol{\tau}_0 + \alpha\bar{\mathbf{n}}, \tag{9}$$

where $\hat{\mathbf{J}}^\top \in \Re^{3\times4}$ is an estimation of $\mathbf{J}^\top$ by assuming uncertainty in the precise measurement of this matrix in practice, $\alpha \in \Re$ is an arbitrary value, which is selected in a way to yield a positive tension for the cables, $\bar{\mathbf{n}} \in \Re^4$ is the null space of the $\hat{\mathbf{J}}^\top$ matrix such that $\hat{\mathbf{J}}^\top\bar{\mathbf{n}} = \mathbf{0}$, and $(\hat{\mathbf{J}}^\top)^\dagger\boldsymbol{\tau}_0$ is the particular solution for the tension, in which $(\hat{\mathbf{J}}^\top)^\dagger \in \Re^{4\times3}$ denotes the pseudo-inverse of $\hat{\mathbf{J}}^\top$ and, $\boldsymbol{\tau}_0 \in \Re^3$ is the applied wrench on the end-effector. With this definition, the following AAN controller is proposed:

$$\boldsymbol{\tau}_0 \triangleq \mathbf{K}_p\mathrm{Tanh}(\gamma\boldsymbol{\varpi}(\mathbf{e})) + \mathbf{K}_d\mathrm{Tanh}(\gamma\boldsymbol{\varpi}(\mathbf{r})) + \hat{\mathbf{f}}, \tag{10}$$

where $\mathbf{K}_p, \mathbf{K}_d \in \Re^{3\times3}$ are diagonal positive-definite gain matrices, and $\hat{\mathbf{f}} \in \Re^3$ is defined in (7), which is a bounded term as it will become clear later. Substituting the controller (10) in (4), considering (8), and adding and subtracting $\boldsymbol{\tau}_0$, the closed-loop dynamics can be written as

$$\begin{aligned}\mathbf{M}\dot{\mathbf{r}} = &-\mathbf{K}_p\mathrm{Tanh}(\gamma\boldsymbol{\varpi}(\mathbf{e})) - \mathbf{K}_d\mathrm{Tanh}(\gamma\boldsymbol{\varpi}(\mathbf{r}))\\ &+ \tilde{\mathbf{W}}^\top\boldsymbol{\sigma}(\mathbf{z}) + \boldsymbol{\varepsilon}(\mathbf{z}) - \mathbf{T}_d + \boldsymbol{\tau}_s\\ &+ \left(\mathbf{I} - \mathbf{J}^\top(\hat{\mathbf{J}}^\top)^\dagger\right)\boldsymbol{\tau}_0 - \alpha\left(\mathbf{J}^\top - \hat{\mathbf{J}}^\top\right)\bar{\mathbf{n}},\end{aligned} \tag{11}$$

where $\mathbf{I} \in \Re^{3\times3}$ denotes a 3×3 identity matrix.

Remark 2: Considering the boundedness property of (10) and assuming that the estimated matrix $\hat{\mathbf{J}}^\top$ is bounded, it is easy to verify that

$$\left\|\left(\mathbf{I} - \mathbf{J}^\top(\hat{\mathbf{J}}^\top)^\dagger\right)\boldsymbol{\tau}_0\right\| \leq \zeta_{J1},$$
$$\left\|\alpha\left(\mathbf{J}^\top - \hat{\mathbf{J}}^\top\right)\bar{\mathbf{n}}\right\| \leq \zeta_{J2},$$

for some positive values of $\zeta_{J1}, \zeta_{J2} \in \Re^+$.

The adaptation law of the NN weight matrix is proposed as follows:

$$\dot{\hat{\mathbf{W}}} \triangleq \mathrm{Proj}\left(\boldsymbol{\Gamma}\boldsymbol{\sigma}(\mathbf{z})\mathbf{r}^\top - \rho\boldsymbol{\Gamma}\hat{\mathbf{W}}\right), \tag{12}$$

where $\boldsymbol{\Gamma} \in \Re^{L\times L}$ is a symmetric positive-definite constant matrix, $\rho \in \Re^+$ is a control gain, and $\mathrm{Proj}(\cdot)$ is a projection operator [37, 38], which is applied to ensure that the estimated weights remain bounded. According to (7), the boundedness of NN weight matrix guarantees the boundedness of $\hat{\mathbf{f}}$.

Remark 3: Similar to the adaptive AAN controllers, e.g. [15], the positive gain ρ in (12) can be considered as a forgetting factor to facilitate the AAN performance, which is primarily used in other robotic applications to give robustness for the estimation of the weight matrix. To clarify its forgetting role, consider the case that the tracking error is small; say $\mathbf{r} \approx 0$. In this condition, according to (12), the weight matrix will exponentially converge to zero, where the decaying rate is adjustable through the gain ρ. From (7), it is obvious that the output level of $\hat{\mathbf{f}}$ will be decreased for small values of the weight matrix. Consequently, when a human subject can follow the desired path, the contribution of this term of controller will be reduced in the generated output wrench.

Now the following theorem is stated for the stability result of the controller:

Theorem 1: Consider the open-loop dynamics of the system defined in (4) with *Assumption* 1 and 2. For bounded initial conditions, let the controller be given through (10) and (7) with the NN weigh update rule defined in (12). The tracking error signals are uniformly ultimately bounded provided the control gain $\mathbf{K}_d$ satisfies the following sufficient condition:

$$\lambda_{\min}(\mathbf{K}_d) > \frac{\kappa_1^2}{4}\left(\chi_{x_h} + \psi_1^{-1}(\rho_2\vartheta^2)\right)^2, \tag{13}$$

where $\lambda_{\min}(\cdot)$ denotes the minimum eigenvalue of a matrix, $\vartheta \in \Re^+$ is defined as $\vartheta \triangleq \max\{d, \|\mathbf{h}(0)\|\}$, and $\kappa_1, \chi_{x_h}, \psi_1(\cdot), d, \rho_2 \in \Re$ and $\mathbf{h} \in \Re^7$ are subsequently defined parameters.

Proof: The following continuously differentiable positive-definite and radially unbounded function is considered to prove the theorem:

$$V \triangleq \int_{\mathbf{0}}^{\mathbf{e}} \mathrm{Tanh}^\top(\gamma\boldsymbol{\varpi}(\bar{\mathbf{e}}))\mathbf{K}_p\mathrm{d}\bar{\mathbf{e}} + \frac{1}{2}\mathbf{r}^\top\mathbf{M}\mathbf{r}$$

$$+\frac{1}{2}\mathrm{tr}\{\tilde{\mathbf{W}}^\top\boldsymbol{\Gamma}^{-1}\tilde{\mathbf{W}}\}, \tag{14}$$

where

$$\int_{\mathbf{0}}^{\mathbf{e}}\mathrm{Tanh}^\top(\gamma\boldsymbol{\varpi}(\bar{\mathbf{e}}))\mathbf{K}_p\mathrm{d}\bar{\mathbf{e}}=\sum_{i=1}^{3}\int_0^{e_i}\tanh(\gamma e_i^3)k_{p_i}\mathrm{d}e_i$$

with $k_{p_i}\in\Re^+$ denoting the i-th component of the diagonal of $\mathbf{K}_p$. Knowing the fact that $\forall\mathbf{x}\in\Re^n$, $1/2\int_{\mathbf{0}}^{\mathbf{x}}\bar{\mathbf{x}}^\top\mathrm{d}\bar{\mathbf{x}}\le\mathbf{x}^\top\mathbf{x}$, and using items (iii), (vii), (viii) and (ix) of Property 3, V can be bounded as

$$\psi_1(\|\mathbf{h}\|)\le V\le\psi_2(\|\mathbf{h}\|), \tag{15}$$

where $\mathbf{h}\triangleq[\mathbf{e}^\top\ \mathbf{r}^\top\ \|\tilde{\mathbf{W}}\|_F]^\top\in\Re^7$, and the functions $\psi_1(\cdot),\psi_2(\cdot):\Re^7\to\Re$ are strictly increasing and radially unbounded non-negative functions, defined as

$$\psi_1(\|\mathbf{h}\|)\triangleq\rho_1\int_0^{\|\mathbf{h}\|}\tanh(\frac{\gamma}{7^{3/2}}\|\bar{\mathbf{h}}\|^3)\mathrm{d}\|\bar{\mathbf{h}}\|,\ \forall\gamma<\gamma_M,$$
$$\psi_2(\|\mathbf{h}\|)\triangleq\rho_2\|\mathbf{h}\|^2,$$

with $\rho_1,\rho_2\in\Re^+$ given by

$$\rho_1\triangleq\min\left\{\lambda_{\min}(\mathbf{K}_p),\ \frac{\lambda_{\min}(\mathbf{M})}{4},\ \frac{\lambda_{\min}(\boldsymbol{\Gamma}^{-1})}{4}\right\},$$
$$\rho_2\triangleq\max\left\{\frac{\gamma^{1/3}\lambda_{\max}(\mathbf{K}_p)}{2},\ \frac{\lambda_{\max}(\mathbf{M})}{2},\ \frac{\lambda_{\max}(\boldsymbol{\Gamma}^{-1})}{2}\right\},$$

where $\lambda_{\max}(\cdot)$ denotes the maximum eigenvalue.

Using (3) and (11), the time derivative of V can be obtained as

$$\begin{aligned}\dot{V}=&-\eta\mathrm{Tanh}^\top(\gamma\boldsymbol{\varpi}(\mathbf{e}))\mathbf{K}_p\mathbf{e}\\&-\mathbf{r}^\top\mathbf{K}_d\mathrm{Tanh}(\gamma\boldsymbol{\varpi}(\mathbf{r}))+\mathbf{r}^\top\left(\mathbf{I}-\mathbf{J}^\top(\hat{\mathbf{J}}^\top)^\dagger\right)\boldsymbol{\tau}_0\\&-\alpha\mathbf{r}^\top\left(\mathbf{J}^\top-\hat{\mathbf{J}}^\top\right)\bar{\mathbf{n}}+\mathbf{r}^\top\boldsymbol{\varepsilon}-\mathbf{r}^\top\mathbf{T}_d+\mathbf{r}^\top\boldsymbol{\tau}_s\\&+\mathrm{tr}\{\tilde{\mathbf{W}}^\top(\boldsymbol{\sigma}(\mathbf{z})\mathbf{r}^\top-\boldsymbol{\Gamma}^{-1}\dot{\hat{\mathbf{W}}})\}.\end{aligned} \tag{16}$$

Using item (iv) of Property 3, assuming $\gamma<\gamma_M$, substituting (12) into (16), and noting the fact that the projection operator in (12) will ensure $\mathrm{tr}\{\tilde{\mathbf{W}}^\top(\boldsymbol{\sigma}(\mathbf{z})\mathbf{r}^\top-\Gamma^{-1}\dot{\hat{\mathbf{W}}})\}\le\mathrm{tr}\{\rho\tilde{\mathbf{W}}^\top\hat{\mathbf{W}}\}$ [39], one can obtain the following upper bound for $\dot{V}$:

$$\begin{aligned}\dot{V}\le&-\eta\lambda_{\min}(\mathbf{K}_p)\|\mathrm{Tanh}(\gamma\boldsymbol{\varpi}(\mathbf{e}))\|^2+\mathrm{tr}\{\rho\tilde{\mathbf{W}}^\top\hat{\mathbf{W}}\}\\&-\lambda_{\min}(\mathbf{K}_d)\|\mathrm{Tanh}(\gamma\boldsymbol{\varpi}(\mathbf{r}))\|^2+\delta\|\mathbf{r}\|,\end{aligned}$$

where $\delta\triangleq\varepsilon_N+\zeta_{J1}+\zeta_{J2}+\zeta_d+\zeta_s$. Note that for $\gamma\ge\gamma_M$, $\|\mathrm{Tanh}(\gamma\boldsymbol{\varpi}(\mathbf{x}))\|$ will be grater than $\|\mathbf{x}\|$ in a small section of trajectories of $\mathbf{x}$, which results in a better stability condition. Now, using item (viii) of Property 3, and the following inequalities:

$$\delta\|\mathbf{r}\|\le\frac{\kappa_1^2}{4}\|\mathbf{r}\|^2+\frac{\delta^2}{\kappa_1^2},$$

$$\begin{aligned}\mathrm{tr}\{\rho\tilde{\mathbf{W}}^\top\hat{\mathbf{W}}\}&\le\rho\|\tilde{\mathbf{W}}\|_F\|\mathbf{W}\|_F-\rho\|\tilde{\mathbf{W}}\|_F^2\\&\le-\left(1-\frac{1}{2\kappa_2^2}\right)\rho\|\tilde{\mathbf{W}}\|_F^2+\frac{1}{2}\kappa_2^2\rho\|\mathbf{W}\|_F^2,\end{aligned}$$

where $\kappa_1\in\Re^+$ and $\kappa_2>\sqrt{2}/2\in\Re^+$ are positive constants, one can write the following upper bound for $\dot{V}$:

$$\begin{aligned}\dot{V}\le&-\eta\lambda_{\min}(\mathbf{K}_p)\tanh^2(\frac{\gamma}{3^{3/2}}\|\mathbf{e}\|^3)\\&-\tanh^2(\frac{\gamma}{3^{3/2}}\|\mathbf{r}\|^3)\left(\lambda_{\min}(\mathbf{K}_d)-\frac{\kappa_1^2\|\mathbf{r}\|^2}{4\tanh^2(\frac{\gamma}{3^{3/2}}\|\mathbf{r}\|^3)}\right)\\&-\left(1-\frac{1}{2\kappa_2^2}\right)\rho\|\tilde{\mathbf{W}}\|_F^2+\beta_1,\end{aligned} \tag{17}$$

where $\beta_1\triangleq\frac{\delta^2}{\kappa_1^2}+\frac{1}{2}\kappa_2^2\rho W_B$ is a bounded constant, which is adjustable through the control gains. If the control gain $\mathbf{K}_d$ satisfies the following condition:

$$\lambda_{\min}(\mathbf{K}_d)>\frac{\kappa_1^2\|\mathbf{r}\|^2}{4\tanh^2(\frac{\gamma}{3^{3/2}}\|\mathbf{r}\|^3)}, \tag{18}$$

then (17) can be written as

$$\dot{V}\le-\psi_3(\|\mathbf{h}\|)+\beta_1, \tag{19}$$

where the strictly increasing non-negative function $\psi_3(\cdot):\Re^7\to\Re$ is defined as $\psi_3(\|\mathbf{h}\|)\triangleq\beta_2\tanh^2(\frac{\gamma}{7^{3/2}}\|\mathbf{h}\|^3)$, in which $\beta_2\in\Re^+$ is given by

$$\begin{aligned}\beta_2\triangleq\min\Bigg\{&\lambda_{\min}(\mathbf{K}_d)-\frac{\kappa_1^2\|\mathbf{r}\|^2}{4\tanh^2(\frac{\gamma}{3^{3/2}}\|\mathbf{r}\|^3)},\\&\eta\lambda_{\min}(\mathbf{K}_p),\left(1-\frac{1}{2\kappa_2^2}\right)\rho\Bigg\}.\end{aligned} \tag{20}$$

To find out a sufficient condition for $\mathbf{K}_d$ to satisfy (18), the outside of the dead-zone area will be considered, while the inside of this area is not of the interest of stability analysis. In other words, inside the dead-zone area the function $\psi_3(\cdot)$ might be negative and V can be increasing accordingly, while outside this area $\psi_3(\cdot)$ will be guaranteed to be non-negative. Therefore, by defining $x_\hbar$ as a value which satisfies $\tanh(\gamma x_\hbar^3)=\hbar$ for some predefined value of $\hbar$, the following inequality can be written outside this area:

$$\frac{\|\mathbf{x}\|}{\tanh(\frac{\gamma}{n^{3/2}}\|\mathbf{x}\|^3)}\le\chi_{x_\hbar}+\|\mathbf{x}\|,\quad\forall\mathbf{x}\in\Re^n, \tag{21}$$

where $\chi_{x_\hbar}\triangleq\sqrt{n}x_\hbar/\tanh(\gamma x_\hbar^3)$. Thus, from (18) and (21), a sufficient condition for $\mathbf{K}_d$ can be obtained as

$$\lambda_{\min}(\mathbf{K}_d)>\frac{\kappa_1^2}{4}\left(\chi_{x_\hbar}+\|\mathbf{h}\|\right)^2$$

for $n=3$. The lower bound on V can be utilized from (15) to state that $\|\mathbf{h}\|\le\psi_1^{-1}(V)$. Consequently, a sufficient condition for $\mathbf{K}_d$ can be written as

$$\lambda_{\min}(\mathbf{K}_d)>\frac{\kappa_1^2}{4}\left(\chi_{x_\hbar}+\psi_1^{-1}(V)\right)^2.$$

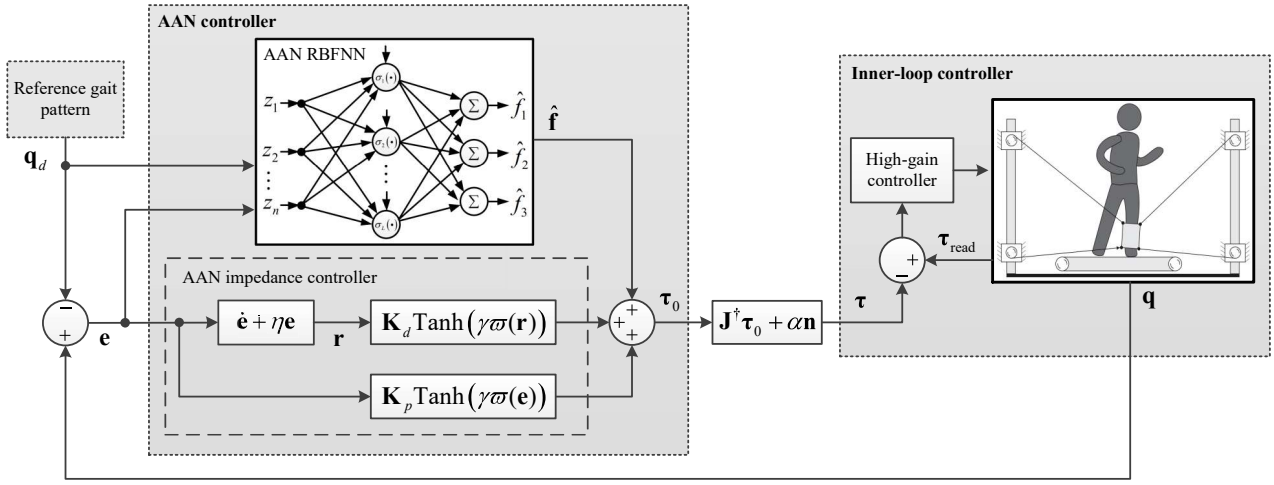

Fig. 3. Block diagram of the proposed control scheme.

Then, similar to the analysis in [40], the final condition for $\mathbf{K}_d$ can be stated as (13).

Now, given (15) and (19), $\mathbf{h}$ is uniformly ultimately bounded in the sense that

$$\|\mathbf{e}(t)\| \le \|\mathbf{h}(t)\| \le d, \quad \forall t \ge T(d, \|\mathbf{h}(0)\|), \tag{22}$$

where $d \in \Re^+$ defines the radius of a ball containing the position tracking error, which can be selected according to [40] as

$$d > \left(\psi_1^{-1} \circ \psi_2\right)\left(\psi_3^{-1}(\beta_1)\right).$$

Also, in (22), $T \in \Re^+$ is a constant that states the time to reach the ball, which is given by

$$T \triangleq \begin{cases} 0, & \|\mathbf{h}(0)\| \le \left(\psi_2^{-1} \circ \psi_1\right)(d), \\ \frac{\psi_2(\|\mathbf{h}(0)\|) - \psi_1\left(\left(\psi_2^{-1} \circ \psi_1\right)(d)\right)}{\psi_3\left(\psi_2^{-1} \circ \psi_1\right)(d) - \beta_1}, & \\ & \|\mathbf{h}(0)\| > \left(\psi_2^{-1} \circ \psi_1\right)(d). \end{cases}$$

□

Remark 4: A different function might be assigned for $\psi_1(\cdot)$ such that its inverse $\psi_1^{-1}(\cdot)$, required in (13), can be analytically expressed. An example is $\psi_1(\|\mathbf{h}\|) = \alpha_1 \log^2(1+\alpha_2\|\mathbf{h}\|^3)$ with $\alpha_1 \triangleq 1/(1+\log(1+\sqrt{\gamma}))$, and $\alpha_2 \triangleq \log(1+\gamma^{2/3})/n^{3/2}$ for all $\gamma \in \Re^+$. For this example, one can obtain $\|\mathbf{h}\| = ((10^{\sqrt{\psi_1(\|\mathbf{h}\|)/\alpha_1}} - 1)/\alpha_2)^{1/3}$.

Remark 5: The controller (9) together with (10) provide *a priori* bounded command, which allows the user to select the control gains $\mathbf{K}_p$ and $\mathbf{K}_d$ such that the stability of the system is guaranteed by meeting the condition (13) and upper limit of the actuators. This concept is similar to many bounded-input controllers in the literature, e.g. [41]. In addition, according to (19) and (20), large values of η, $\mathbf{K}_p$ and $\mathbf{K}_d$ will decrease the tracking error outside the dead-zone area, which will result in a stiff control system outside this area.

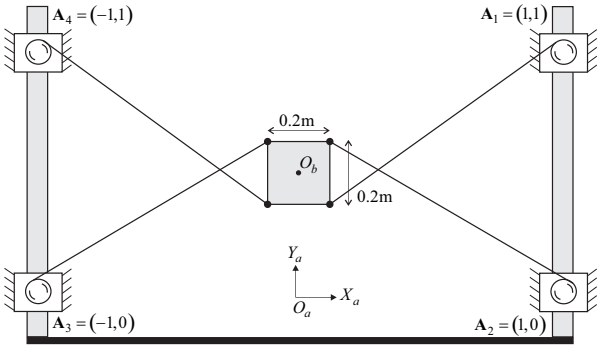

Fig. 4. Configuration of the studied 4-cable planar parallel robot.

Block diagram of the proposed control scheme is demonstrated in Fig. 3.

4. SIMULATION RESULTS

In this section, the effectiveness of the proposed AAN controller is evaluated through simulations. Simulations are performed in MATLAB 2016a and its Simulink environment. The geometrical structure and configuration of the studied 4-cable planar robot is shown in Fig. 4. The cross configuration for the cables is utilized in order to increase the wrench-closure workspace of the robot. Following [27], the dynamics of the robot in (1) is simulated with the assumption that the Coulomb friction and unmodeled dynamics terms are negligible comparing to the other terms. An NN with 9 neurons is used to estimate the function $\mathbf{f}$. For this network p_i is set at 50 for all activation function, and the centers μ_i are evenly spaced in $[-7\ 7]$. The value of parameters of the dynamic model, together

Table 1. Simulation parameters.

Parameter	Value	Unit
m	6	kg
I	0.05	$\mathrm{kg\,m^2}$
g	9.81	$\mathrm{m\,s^{-2}}$
$\mathbf{F}_d$	$\mathrm{diag}\{0.5,0.5,0.5\}$	$\frac{\mathrm{kg}}{\mathrm{s}}, \frac{\mathrm{kg\,m^2}}{\mathrm{s}}$
η	0.4	–
γ	120	–
$\mathbf{K}_p$	$\mathrm{diag}\{50,50,0.2\}$	–
$\mathbf{K}_d$	$\mathrm{diag}\{150,150,1\}$	–
$\mathbf{\Gamma}$	$\mathrm{diag}\{12,\cdots,12\}$	–

with that of controller gains are given in Table 1.

The desired gait pattern is simulated based on a model given in [42], which has a gait cycle of three seconds. The controller is assumed to move the end-effector such that the shank follows the desired trajectory with an AAN behaviour. 2D position information of the end-effector as well as the orientation of it in the sagittal plane are assumed to be obtained through a visual sensor, as reported in [43].

In the first simulation, the performance of the controller is analysed for the case that the human subject cannot apply the desired wrench, necessary to follow the trajectory. Here, the navigating input is only exerted by the controller, while the effect of the subject force is modeled by 10% of the desired force applied in the opposite direction. The value of the forgetting factor ρ is set at 0.0001 in this simulation. Fig. 5 illustrates the desired gait pattern, and the end-effector trajectory in the X_aY_a plane. The norm of error signals for one gaite cycle is shown in Fig. 6. The applied tension forces in the four cables are illustrated in Fig. 7. Also, Fig. 8 and Fig. 9 respectively show the time evolution of the estimation of the function $\mathbf{f}$ and the weight matrix $\mathbf{W}$. The results demonstrate a stable tracking performance with a reasonable tracking error, generated mainly due to the assigned dead-zone area.

In the second simulation, it is assumed that the subject can exert the required wrench to follow the trajectory with small deviation. This wrench is generated through the output of controller of another simulated model. To amplify the AAN property of the RBFNN, the value of ρ is increased in this simulation and set at 0.1. The trajectory of the end-effector in the X_aY_a plane is shown in Fig. 10. The error signals are illustrated in Fig. 11. The time evolution of the exerted $\hat{\mathbf{f}}$ function is shown in Fig. 13, and Fig. 14 shows the estimation of the weight matrix $\mathbf{W}$. It is obvious from these figures that the applied forces by the NN term decrease rapidly toward zero, due to the small tracking error and high-gain forgetting factor. Also Fig. 12 illustrates the tension forces of the cables during one gait cycle.

To compare the AAN performance of the proposed controller with the existing ones, in the third simulation the

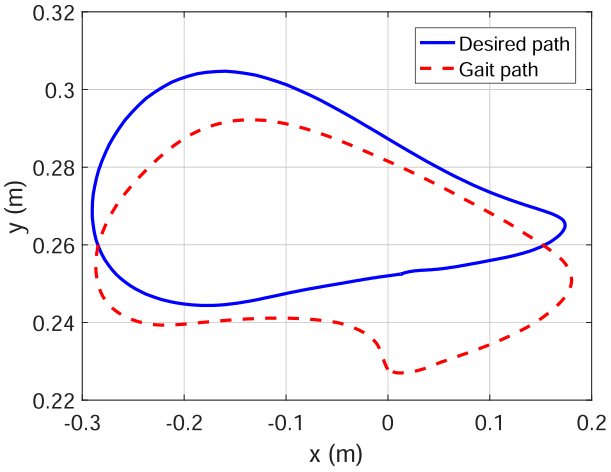

Fig. 5. Simulation 1: Desired path and end-effector's trajectory in X_aY_a plane.

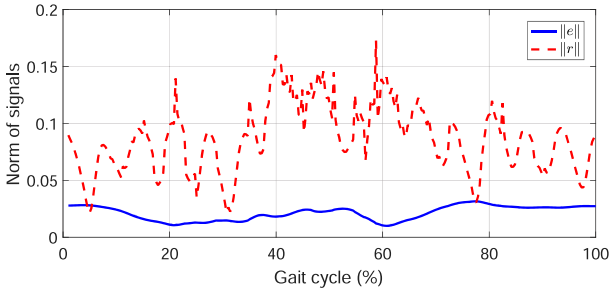

Fig. 6. Simulation 1: Norm of tracking errors in one gait cycle.

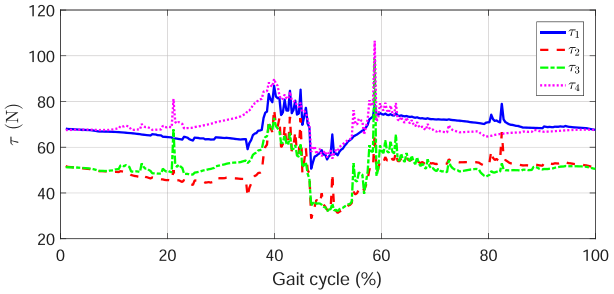

Fig. 7. Simulation 1: Cables' tension in one gait cycle.

following PD-type controller is utilized:

$$\boldsymbol{\tau}_0 = \mathbf{K}_p\mathbf{e} + \mathbf{K}_d\mathbf{r} + \hat{\mathbf{f}}, \tag{23}$$

where the function $\hat{\mathbf{f}}$ is estimated through the proposed RBFNN in this paper. Similar to the second simulation, it is assumed that the human subject can apply the desired wrench to follow the gait pattern. The norm of the wrench generated with this controller, during one gait cycle, is compared in Fig. 15 with that of the proposed one in this paper. This figure demonstrates higher intervention

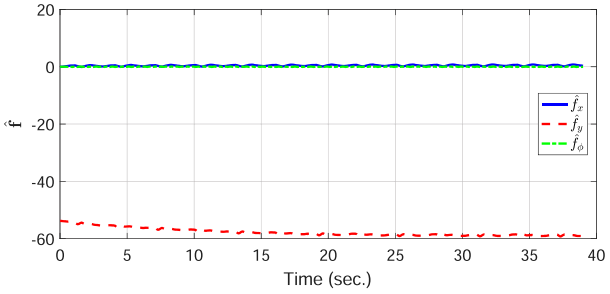

Fig. 8. Simulation 1: Time evolution of the estimation of $\hat{\mathbf{f}} = [\hat{f}_x\ \hat{f}_y\ \hat{f}_\phi]^\top$.

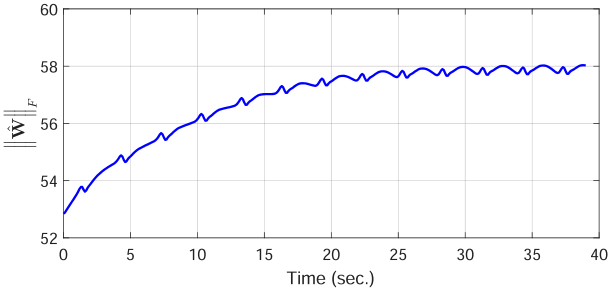

Fig. 9. Simulation 1: Time evolution of norm of estimation of $\mathbf{W}$.

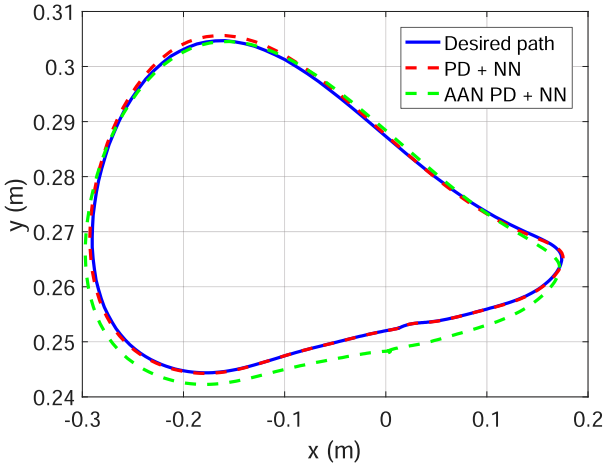

Fig. 10. Simulation 2: Desired path and end-effector's trajectory in X_aY_a plane.

of the classic PD AAN controller when the subject can generate the desired wrench. As a numerical comparison, the integral of the norm of τ_0 is computed for two methods within one gait cycle, where the results show 230% higher value for the PD controller. The trajectory of the end-effector in X_aY_a plane for the PD controller is also illustrated in Fig. 16, which shows that the higher wrench is produced even for a smaller position tracking error.

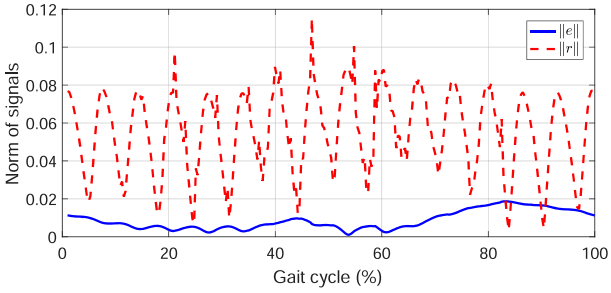

Fig. 11. Simulation 2: Norm of tracking errors in one gait cycle.

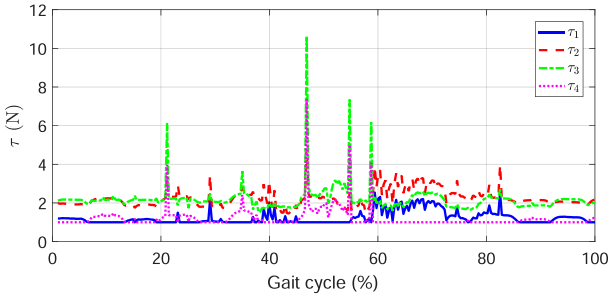

Fig. 12. Simulation 2: Cables' tension in one gait cycle.

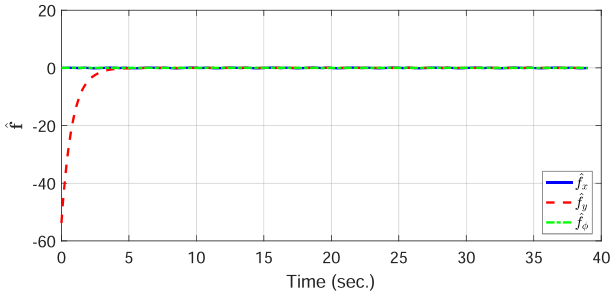

Fig. 13. Simulation 2: Time evolution of the estimation of $\hat{\mathbf{f}}$.

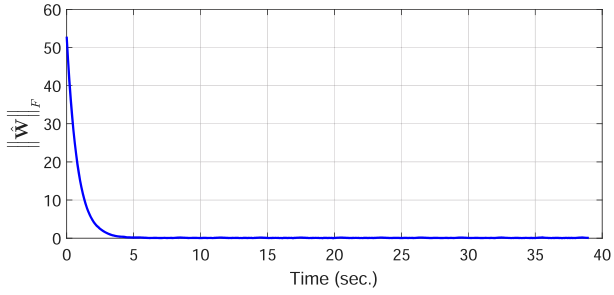

Fig. 14. Simulation 2: Time evolution of norm of estimation of $\mathbf{W}$.

5. CONCLUSION

The problem of AAN controller design has been studied in this paper. The proposed control law consists of

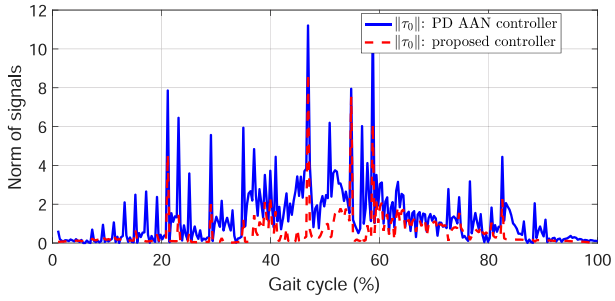

Fig. 15. Simulation 3: Comparison of the norm of τ_0 for the PD AAN controller (23) and the proposed controller.

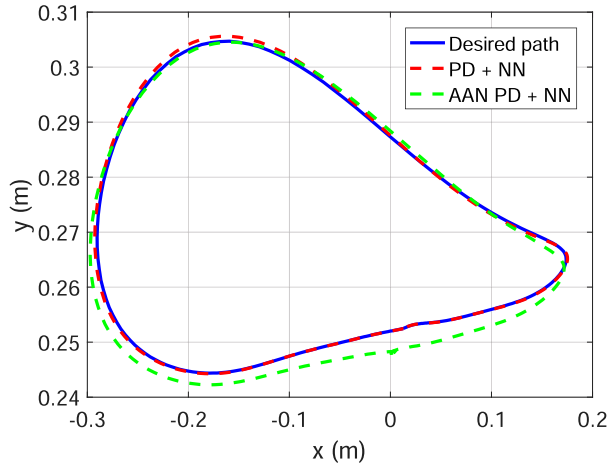

Fig. 16. Simulation 3: Desired path and end-effector's trajectory in X_aY_a plane for two studied methods.

a bounded AAN impedance term, which provides an adjustable tunnel of freedom around the desired trajectory. The controller also includes an RBFNN to compensate for the unknown dynamics of the system. This term also possesses the AAN property with an adjustable level through a control gain. These features increase the AAN property of the existing model-based controllers. Simulation results of the proposed controller show a clear improvement in the performance, as a satisfactory wrench level is obtained by the robot when the human subject can follow the desired movement pattern.

The future work is devoted to test the performance of the controller in practice on a real robot. Also, it is intended to verify the effectiveness of the proposed approach on patients with various levels of injury.

REFERENCES

[1] C. Bütefisch, H. Hummelsheim, P. Denzler, and K.-H. Mauritz, "Repetitive training of isolated movements improves the outcome of motor rehabilitation of the centrally paretic hand," *Journal of the Neurological Sciences*, vol. 130, no. 1, pp. 59-68, 1995. [click]

[2] R. Riener, T. Nef, and G. Colombo, "Robot-aided neurorehabilitation of the upper extremities," *Medical and Biological Engineering and Computing*, vol. 43, no. 1, pp. 2-10, 2005.[click]

[3] L. Marchal-Crespo and D. J. Reinkensmeyer, "Review of control strategies for robotic movement training after neurologic injury," *Journal of Neuroengineering and Rehabilitation*, vol. 6, no. 1, 2009.

[4] Y. Mao and S. K. Agrawal, "Design of a cable-driven arm exoskeleton (carex) for neural rehabilitation," *IEEE Transactions on Robotics*, vol. 28, no. 4, pp. 922-931, 2012. [click]

[5] S. K. Banala, S. K. Agrawal, and J. P. Scholz, "Active leg exoskeleton (alex) for gait rehabilitation of motor-impaired patients," *Proc. of IEEE 10th International Conference on Rehabilitation Robotics*, pp. 401-407, 2007. [click]

[6] G. Colombo, M. Joerg, R. Schreier, and V. Dietz, "Treadmill training of paraplegic patients using a robotic orthosis," *Journal of Rehabilitation Research and Development*, vol. 37, no. 6, p. 693, 2000.

[7] R. Riener, L. Lunenburger, S. Jezernik, M. Anderschitz, G. Colombo, and V. Dietz, "Patient-cooperative strategies for robot-aided treadmill training: first experimental results," *IEEE Transactions on Neural Systems and Rehabilitation Engineering*, vol. 13, no. 3, pp. 380-394, 2005. [click]

[8] E. T. Wolbrecht, J. Leavitt, D. J. Reinkensmeyer, and J. E. Bobrow, "Control of a pneumatic orthosis for upper extremity stroke rehabilitation," *Proc. of 28th Annual International Conference of the IEEE Engineering in Medicine and Biology Society*, 2006, pp. 2687-2693.

[9] N. Hogan, H. I. Krebs, B. Rohrer, J. J. Palazzolo *et al.*, "Motions or muscles? some behavioral factors underlying robotic assistance of motor recovery," *Journal of rehabilitation research and development*, vol. 43, no. 5, pp. 605-618, 2006. [click]

[10] J. L. Emken, J. E. Bobrow, and D. J. Reinkensmeyer, "Robotic movement training as an optimization problem: designing a controller that assists only as needed," in *9th International Conference on Rehabilitation Robotics*, pp. 307-312.

[11] D. J. Reinkensmeyer, D. Aoyagi, J. L. Emken, J. A. Galvez *et al.*, "Tools for understanding and optimizing robotic gait training," *Journal of Rehabilitation Research and Development*, vol. 43, no. 5, p. 657, 2006. [click]

[12] L. L. Cai, A. J. Fong, C. K. Otoshi, Y. Liang, J. W. Burdick, R. R. Roy, and V. R. Edgerton, "Implications of assist-as-needed robotic step training after a complete spinal cord injury on intrinsic strategies of motor learning," *The Journal of Neuroscience*, vol. 26, no. 41, pp. 10 564-10 568, 2006.

[13] S. Srivastava, P.-C. Kao, S. H. Kim, P. Stegall, D. Zanotto, J. S. Higginson, S. K. Agrawal, and J. P. Scholz, "Assist-as-needed robot-aided gait training improves walking function in individuals following stroke," *IEEE Transactions on Neural Systems and Rehabilitation Engineering*, vol. 23, no. 6, pp. 956-963, 2015. [click]

[14] A. Duschau-Wicke, J. von Zitzewitz, A. Caprez, L. Lunenburger, and R. Riener, "Path control: a method for patient-cooperative robot-aided gait rehabilitation," *IEEE Transactions on Neural Systems and Rehabilitation Engineering*, vol. 18, no. 1, pp. 38-48, 2010. [click]

[15] E. T. Wolbrecht, V. Chan, D. J. Reinkensmeyer, and J. E. Bobrow, "Optimizing compliant, model-based robotic assistance to promote neurorehabilitation," *IEEE Transactions on Neural Systems and Rehabilitation Engineering*, vol. 16, no. 3, pp. 286-297, 2008. [click]

[16] A. U. Pehlivan, F. Sergi, and M. K. O'Malley, "A subject-adaptive controller for wrist robotic rehabilitation," *IEEE/ASME Transactions on Mechatronics*, vol. 20, no. 3, pp. 1338-1350, 2015. [click]

[17] S. Fang, D. Franitza, M. Torlo, F. Bekes, and M. Hiller, "Motion control of a tendon-based parallel manipulator using optimal tension distribution," *IEEE/ASME Transactions on Mechatronics*, vol. 9, no. 3, pp. 561-568, 2004. [click]

[18] S. Kawamura, H. Kino, and C. Won, "High-speed manipulation by using parallel wire-driven robots," *Robotica*, vol. 18, no. 01, pp. 13-21, 2000. [click]

[19] G. Abbasnejad, J. Yoon, and H. Lee, "Optimum kinematic design of a planar cable-driven parallel robot with wrench-closure gait trajectory," *Mechanism and Machine Theory*, vol. 99, pp. 1-18, 2016. [click]

[20] K. Homma, O. Fukuda, J. Sugawara, Y. Nagata, and M. Usuba, "A wire-driven leg rehabilitation system: development of a 4-dof experimental system," *Proc. of IEEE/ASME International Conference on Advanced Intelligent Mechatronics*, vol. 2, pp. 908-913, 2003. [click]

[21] M. Wu, T. G. Hornby, J. M. Landry, H. Roth, and B. D. Schmit, "A cable-driven locomotor training system for restoration of gait in human sci," *Gait & posture*, vol. 33, no. 2, pp. 256-260, 2011. [click]

[22] X. Jin, X. Cui, and S. K. Agrawal, "Design of a cable-driven active leg exoskeleton (c-alex) and gait training experiments with human subjects," *Proc. of IEEE International Conference on Robotics and Automation*, pp. 5578-5583, 2015.

[23] J. Yang, H. Su, Z. Li, D. Ao, and R. Song, "Adaptive control with a fuzzy tuner for cable-based rehabilitation robot," *International Journal of Control, Automation and Systems*, vol. 14, no. 3, pp. 865-875, 2016. [click]

[24] P. Bosscher, A. T. Riechel, and I. Ebert-Uphoff, "Wrench-feasible workspace generation for cable-driven robots," *IEEE Transactions on Robotics*, vol. 22, pp. 890-902, 2006. [click]

[25] M. Gouttefarde and C. M. Gosselin, "Analysis of the wrench-closure workspace of planar parallel cable-driven mechanisms," *IEEE Transactions on Robotics*, vol. 22, no. 3, pp. 434-445, 2006. [click]

[26] R. L. Williams, P. Gallina, and J. Vadia, "Planar translational cable-direct-driven robots," *Journal of Robotic Systems*, vol. 20, no. 3, pp. 107-120, 2003. [click]

[27] M. A. Khosravi and H. D. Taghirad, "Robust PID control of fully-constrained cable driven parallel robots," *Mechatronics*, vol. 24, no. 2, pp. 87-97, 2014.

[28] J. Seok, W. Yoo, and S. Won, "Inertia-related coupling torque compensator for disturbance observer based position control of robotic manipulators," *International Journal of Control, Automation and Systems*, vol. 10, no. 4, pp. 753-760, 2012. [click]

[29] X.-Y. Wen, L. Guo, and P. Yan, "Composite hierarchical anti-disturbance control for robotic systems with multiple disturbances," *International Journal of Control, Automation and Systems*, vol. 12, no. 3, pp. 541-551, 2014. [click]

[30] H. Medellin, J. Corney, J. Ritchie, and T. Lim, "Automatic generation of robot and manual assembly plans using octrees," *Assembly Automation*, vol. 30, no. 2, pp. 173-183, 2010.

[31] S.-I. Han and J.-M. Lee, "Adaptive fuzzy backstepping dynamic surface control for output-constrained non-smooth nonlinear dynamic system," *International Journal of Control, Automation and Systems*, vol. 10, no. 4, pp. 684-696, 2012.

[32] S. M. Tabatabaei and M. M. Arefi, "Adaptive neural control for a class of uncertain non-affine nonlinear switched systems," *Nonlinear Dynamics*, vol. 83, no. 3, pp. 1773-1781, 2016. [click]

[33] F. Lewis, S. Jagannathan, and A. Yesildirak, *Neural Network Control of Robot Manipulators and Non-linear Systems*, CRC Press, 1998.

[34] M. M. Arefi and M. R. Jahed-Motlagh, "Observer-based adaptive neural control for a class of nonlinear non-affine systems with unknown gain sign," *IFAC Proceedings Volumes*, vol. 44, no. 1 , pp. 2644-2649, 2011.

[35] S.-I. Han and J.-M. Lee, "Decentralized neural network control for guaranteed tracking error constraint of a robot manipulator," *International Journal of Control, Automation and Systems*, vol. 13, no. 4, pp. 906-915, 2015. [click]

[36] E. Aguiñaga-Ruiz, A. Zavala-Río, V. Santibáñez, and F. Reyes, "Global trajectory tracking through static feedback for robot manipulators with bounded inputs," *IEEE Transactions on Control Systems Technology*, vol. 17, pp. 934-944, 2009. [click]

[37] H. Jabbari Asl, G. Oriolo, and H. Bolandi, "An adaptive scheme for image-based visual servoing of an underactuated Uav," *International Journal of Robotics and Automation*, vol. 29, 2014.

[38] H. J. Asl and J. Yoon, "Adaptive vision-based control of an unmanned aerial vehicle without linear velocity measurements," *ISA Transactions*, vol. 65, pp. 296-306, 2016.

[39] P. M. Patre, W. MacKunis, K. Kaiser, and W. E. Dixon, "Asymptotic tracking for uncertain dynamic systems via a multilayer neural network feedforward and rise feedback control structure," *IEEE Transactions on Automatic Control*, vol. 53, no. 9, pp. 2180-2185, 2008. [click]

[40] N. Fischer, A. Dani, N. Sharma, and W. Dixon, "Saturated control of an uncertain nonlinear system with input delay," *Automatica*, vol. 49, no. 6, pp. 1741-1747, 2013. [click]

[41] W. E. Dixon, M. S. de Queiroz, F. Zhang, and D. M. Dawson, "Tracking control of robot manipulators with bounded torque inputs," *Robotica*, vol. 17, no. 02, pp. 121-129, 1999.

[42] C. L. Vaughan and B. L. Davis, *Dynamics of Human Gait*.

[43] R. Babaghasabha, M. A. Khosravi, and H. D. Taghirad, "Adaptive robust control of fully-constrained cable driven parallel robots," *Mechatronics*, vol. 25, pp. 27-36, 2015. [click]

Hamed Jabbari Asl received the Ph.D. in Electrical Engineering in 2013 from Iran University of Science and Technology. In 2011-2012 he was a visiting scholar at the Dipartimento di Informatica e Sistemistica, Universita di Roma "La Sapienza", and in 2015-2016 he was a Senior Researcher at Robots & Intelligent Systems Lab, Gyeongsang National University. Currently, he is postdoctoral fellow at Toyota Technological Institute. His research interests include robot-aided rehabilitation, and nonlinear control applications.

Jungwon Yoon received the Ph.D. degree in the Department of Mechatronics, Gwangju Institute of Science and Technology (GIST), Gwangju, Korea, in 2005. He was a Senior Researcher in Electronics Telecommunication Research Institute (ETRI), Daejeon, Korea. From 2001 to 2002, he was a Visiting Researcher at Virtual Reality Lab, Rutgers University, Piscataway, NJ, USA, and was a Visiting Fellow at Functional and Applied Biomechanics Section, Rehabilitation Medicine of Department, Clinical Center, National Institutes of Health, Bethesda,MD, USA, from 2010 to 2011. From 2005 to 2017, he was a professor in the School of Mechanical and Aerospace Engineering, Gyeongsang National University, Jinju, Korea. In 2017, he joined the School of Integrated Technology, Gwangju Institute of Science and Technology, Gwangju, Korea, where he is currently an Associate Professor. His current research interests include bio-nano robot control, virtual reality haptic devices, and rehabilitation robots. He has authored or coauthored more than 70 peer-reviewed journal articles and patents.